Hyperspherical analysis of radial correlations in four-electron atoms

Toru Morishita[1] and C. D. Lin[2]
[1]*Department of Applied Physics and Chemistry, University of Electro-Communications, 1-5-1 Chofu-ga-oka, Chofu-shi, Tokyo 182-8585, Japan*
[2]*Department of Physics, Kansas State University, Manhattan, Kansas 66506, USA and Physics Division, National Center for Theoretical Sciences, P. O. Box 2-131, Hsinchu, 30013, Taiwan*
(Received 8 April 2004; published 20 January 2005)

Hyperspherical coordinates are used to study electron correlations in the radial motion of a four-electron atom within the model of s^4 configurations. We identify groups of hyperspherical adiabatic potential curves that support singly, doubly, triply, and quadruply excited states. By examining the nodal structures of the channel functions, we show that it is possible to relate the number of nodal surfaces in the hyperangles and the principal quantum numbers used in the independent particle picture.

DOI: 10.1103/PhysRevA.71.012504 PACS number(s): 31.15.Ja, 31.10.+z, 31.25.−v, 31.30.−i

I. INTRODUCTION

Since the advent of quantum mechanics, the description of a many-electron atom is based mostly on the independent particle model (IPM). Within this model, a many-electron atomic state is designated by a collection of quantum numbers from the individual electrons. However, in the past few decades extensive theoretical and experimental investigations of doubly excited states and, to a lesser extent, triply excited states of atoms have revealed that the independent particle model is inadequate. At the next level of complexity, one can expect that the IPM also would not work for quadruply excited states. However, little is known about them, both experimentally and theoretically. Unlike doubly and triply excited states where approximate new quantum numbers have been identified, little has been done for the classification of quadruply excited states.

For multiply excited states, the motions of the electrons are highly correlated and they are better described as analogous to the rotation and vibration of a polyatomic molecule. Thus doubly excited states of a two-electron atom can be described qualitatively in terms of the rovibrational motion of a linear XY_2 molecule, where X stands for the nucleus and Y for the electron [1–9]. Various theoretical approaches have come to similar conclusions and this subject has been reviewed extensively, for example, most recently by Rost *et al.* [10], and within the semiclassical method by Tanner *et al.* [11]. Similarly, triply excited states of an atom can be described in terms of the rovibrational motion of a symmetric top XY_3 molecule [12–17], mostly based on the hyperspherical approach. Except for the symmetric rotor states which have been constructed using the algebraic approach (see the review by Madsen [18]), most of the other approaches for doubly excited states have not been extended to triply excited states. These qualitative descriptions of the rovibrational modes are supported by analyzing the actual calculated wave functions, and the nodal surfaces of the wave functions of doubly and triply excited states are related to the new quantum numbers that describe the collective normal modes of the joint motion of the electrons [7,8,16,17]. It is natural to ask if the theoretical tools developed for doubly and triply excited states of atoms can be extended to analyzing quadruply excited states of atoms where one can expect much richer electron correlation effects. A new classification scheme and a new set of quantum numbers will be needed eventually for describing quadruply excited states as well. However, this is a monumental task, and before such a scheme is possible, the various aspects of the correlated motions of the four electrons should be examined in pieces first. Experimentally, little is known about the quadruply excited states of an atom, although attempts are being made on these states for the beryllium atom using synchrotron radiation [19]. Such states are also formed in collisions of multiply charged ions with multielectron targets, but they have not been identified individually due to the lack of enough energy resolution.

In the electronic structure of an atomic system, the motion in angular variables and that in radial variables are approximately separated in the energy spectra at least for the lower excited states. Thus the angular and radial correlations in atoms can be considered separately. Indeed, the procedure developed for classifying doubly and triply excited states has followed these two steps. First, a new classification scheme is developed for intrashell states where all the electrons are at about the same distance from the nucleus. To simplify the study of these intrashell states, they are often analyzed by an approximate model atom where all the electrons are confined to the surface of a sphere [6,12,13,16]. This has the advantage that one can deal with doubly excited states of a two-electron atom directly without calculating singly excited states, or deal with triply excited states of a three-electron atom directly without the need of calculating the lower singly and doubly excited states. For quadruply excited states, a similar analysis within this model has been investigated by Bao and co-workers in a series of papers [20–23]. In their papers, the nodal structures stemming from quantum symmetries for a subset of intrashell quadruply excited states have been examined for different L, S, and π, the total orbital and angular momenta and parity, respectively. It was shown that, similarly to doubly and triply intrashell states, the energy levels of intrashell quadruply excited states can be ordered according to the number of nodal surfaces of the wave functions, at least for the lower quadruply excited states. The four-electron system is the first few-electron system that has

more than one equilibrium configuration in the intrashell states. One is a tetrahedron with the four electrons at the corners and the nucleus at the center; the other is a coplanar square with the nucleus at the center. In their papers, these two configurations have been identified for the four-electron states on the surface of a sphere. Komninos and Nicolaidas [24] also calculated the angle between two electrons for the type of $nsnp^{3}S^{o}$ intrashell quadruply excited states by the multiconfigurational Hartree-Fock method, from which they confirmed that the electron densities of these intrashell states indeed reveal a tetrahedron shape.

The second step in the classification of multiply excited states is to focus on intershell states. For such states, the electrons are located mostly at different distances from the nucleus. The joint radial motion of two such electrons is distinguished by the so-called "+" and "−" quantum numbers initially introduced by Fano and co-workers [1]. The "+" corresponds to the mechanical analog that the two electrons move toward or away from the nucleus together with the same phase, and the "−" with opposite phase. The concept of "+" and "−" has been extended by us to describe intershell triply excited states recently [17]. To examine the radial motion in intershell quadruply excited states, for the time being one can average out the angular degrees of freedom to simplify the calculation and analysis. Thus in the present paper, we address quadruply excited states within the s^4 configuration, where the orbital angular momentum of each electron is set to zero, similar to the analysis of the three-electron atom in the s^3 configuration [25–27]. With this model, we also set out to separate singly, doubly, triply, and quadruply excited states of a four-electron atom from the whole spectrum of the four-electron Hamiltonian. Since the spins of the four s electrons can couple to form total spin $S=0$, 1, and 2, we will examine how these states depend on the total spin of the system.

We will use hyperspherical coordinates for the study of the four-electron atoms. This paper serves two purposes. First, we develop the theoretical and computational techniques needed for studying a four-electron atom using the hyperspherical approach. No previous work using hyperspherical coordinates has been applied to four-electron atoms except for the general analysis of hyperspherical harmonics by Cavagnero [28–30]. Conceptually the method is similar to that for the two-electron and three-electron atoms, but the computational complexity is a good step forward. Second, we focus on the analysis of radial correlations among the four electrons. Thus the present work complements the analysis of angular correlations studied by Bao and coworkers.

The rest of this paper is organized as follows. In Sec. II we express the Schrödinger equation in hyperspherical coordinates, characterized by a hyperradius and three hyperangles. There are two obvious different methods of choosing the hyperangles, and we study the properties of the two sets of coordinate systems, considering the permutation symmetry of the four electrons. Choosing the hyperradius as an adiabatic parameter, we obtained the adiabatic potential curves and the associated channel functions. In Sec. III we examine these potential curves to identify groups of curves that support singly, doubly, triply, and quadruply excited states in the s^4 configuration. In Sec. IV, we analyze the channel functions. Within the s^4 configuration, we show that it is possible to relate the principal quantum numbers in the IPM to the number of nodal surfaces in the hyperangles. Even though the calculation was carried out in the s^4 configuration, this conclusion is expected to be the same for real atoms where angular correlation is included. We end this paper with a short summary and perspective for future development.

Atomic units are used throughout in this paper.

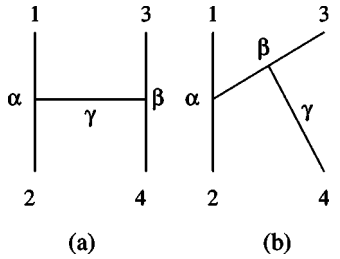

FIG. 1. Schematic diagram of the hyperspherical coordinates for four-electron atoms. (a) H set: α measures the relative distance between electrons 1 and 2, β measures the relative distance between electrons 3 and 4, and the relative distance between pair (1,2) and pair (3,4) is measured by γ. (b) K set: Electrons 1, 2, 3, and 4 are coupled one by one in a hierarchical order.

II. HYPERSPHERICAL METHOD FOR FOUR-ELECTRON ATOMS

A. The choice of hyperangles

Following the procedure for two- and three-electron atoms used previously we will employ hyperspherical coordinates to describe the four-electron atoms. Instead of the four radial distances of the electrons from the nucleus, r_1, r_2, r_3, and r_4, we define a hyperradius $R=\sqrt{r_1^2+r_2^2+r_3^2+r_4^2}$, which characterizes the size of the system, and three hyperangles α, β, and γ, measuring the relative distances among the four electrons. Two alternative sets of hyperangles can be defined as

$$\left.\begin{aligned} r_1 &= R\cos\gamma\cos\alpha \\ r_2 &= R\cos\gamma\sin\alpha \\ r_3 &= R\sin\gamma\cos\beta \\ r_4 &= R\sin\gamma\sin\beta \end{aligned}\right\} \text{(H set)} \tag{1}$$

and

$$\left.\begin{aligned} r_1 &= R\sin\gamma\sin\beta\sin\alpha \\ r_2 &= R\sin\gamma\sin\beta\cos\alpha \\ r_3 &= R\sin\gamma\cos\beta \\ r_4 &= R\cos\gamma \end{aligned}\right\} \text{(K set)}. \tag{2}$$

The range of the hyperangles for both sets is $0\leqslant\alpha,\beta,\gamma\leqslant\pi/2$. Schematically these two sets are indicated in Fig. 1. In the H set, α measures the relative distance between electrons 1 and 2, while β measures the relative distances between electrons 3 and 4. The relative distance between pair

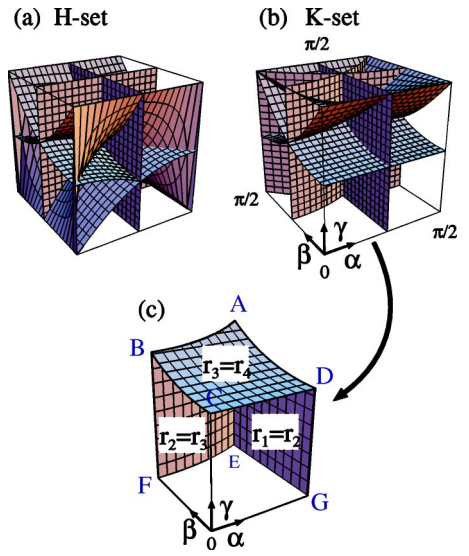

FIG. 2. (a) Division of the 24 equivalent domains of the radial configuration space in the space of three hyperangles of a four-electron atom in the H set. (b) The same as (a) but in the K set. (c) The domain of $r_1 \leqslant r_2 \leqslant r_3 \leqslant r_4$ in the K set.

(1,2) and pair (3,4) is measured by the angle γ. In the K set, the electrons are coupled one by one in a hierarchical order. The first two electrons 1 and 2 are coupled through α, and electron 3 is coupled to this (1,2) pair through β, and then electron 4 is coupled to the three electrons through γ. For convenience, we shall use Ω to denote the hyperangles (α,β,γ) collectively. When we specify the hyperangles in the H set or the K set, we use Ω_{H} or Ω_{K}, respectively.

Since the electrons are indistinguishable, the spatial part of the wave function can be divided into $4!=24$ physically equivalent domains separated by the surfaces where two of the individual radii r_i coincide. In Fig. 2 we show these 24 domains of the three-dimensional (3D) space of the hyperangles (α,β,γ), in the H set and in the K set, respectively. It is sufficient to consider only one of the 24 domains. In principle, one can solve the Schrödinger equation within a domain with certain symmetry conditions on the boundaries and then extend the wave function to the whole configuration space using the projection operators of the S_4 permutation group. However, the boundary surfaces are not separable with respect to the hyperspherical variables for both sets. It is more convenient to choose a particular set for the calculation, but for illustration and for visualizing the results, display using the other set of coordinates may be more transparent.

Let us examine the two sets of coordinates more precisely. The properties of the K set and the H set coordinates can be easily seen in the plots of the boundary surfaces in the hyperangular space. In the H set, particle permutations of (12), (34), and (13)(24) are represented by the exchange of the angles $\alpha \leftrightarrow \pi/4-\alpha$, $\beta \leftrightarrow \pi/4-\beta$, and $\gamma \leftrightarrow \pi/4-\gamma$ with $\alpha \leftrightarrow \beta$, respectively. Clearly we can see these exchange symmetries in Fig. 2(a) as the structure of the boundary surfaces of the reflections with respect to the two flat planes of $\alpha=\pi/4$ and $\beta=\pi/4$, and space inversion with respect to the center of $\alpha=\beta=\gamma=\pi/4$. Using these symmetry properties, appropriate boundary conditions in the coordinate space can be easily incorporated to reduce the Hilbert space by 1/8. In the K set, however, the size of the space is reduced by only 1/2 using (12), represented by the symmetry of $\alpha \leftrightarrow \pi/4-\alpha$. Thus we use the H set coordinates in the actual numerical calculations of the channel functions. Meanwhile, the analysis of the wave functions will be presented in the K set coordinates, since it is easier to analyze the hierarchical nodal structure of the wave functions in the hyperangles (α,β,γ) in this set, and to see the relation between the hyperspherical coordinates and the independent particle coordinates. Only one of the 24 domains is sufficient to analyze the wave function. We will use the domain in the K set which covers the space in hierarchical order of radii r_i, $r_1 \leqslant r_2 \leqslant r_3 \leqslant r_4$. We show this domain in Fig. 2(c). On each two-dimensional boundary surface that separates two neighboring domains, two electrons are at the same distance from the nucleus. The surfaces containing *ABCD*, *AEGD*, and *ABFE* are for $r_1 \leqslant r_2 \leqslant r_3 = r_4$, $r_1 = r_2 \leqslant r_3 \leqslant r_4$, and $r_1 \leqslant r_2 = r_3 \leqslant r_4$, respectively. Similarly, on each line where two of these boundary surfaces coincide, three electrons or two pairs of two electrons are at the same distance. The curve *AB* is for $r_1 \leqslant r_2 = r_3 = r_4$, and the curve *AE* is for $r_1 = r_2 = r_3 \leqslant r_4$, while the curve *AD* is for $r_1 = r_2 \leqslant r_3 = r_4$. The point *A*, where the three boundary lines coincide, represents the case where all the four electrons are at the same distance from the nucleus. The 2D surfaces of *ABCD* and *ABFE* are almost flat, so that the nodal structures can be clearly seen with respect to the hyperangles in this domain.

B. The Schrödinger equation

The Schrödinger equation for a four-electron atom in terms of independent electron coordinates with the nucleus at the center is

$$\left[\sum_{i=1}^{4}\left(-\frac{1}{2}\Delta_i^2+\frac{Z}{r_i}\right)+\sum_{i>j}\frac{1}{|\mathbf{r}_i-\mathbf{r}_j|}-E\right]\Psi=0, \tag{3}$$

where E is the total energy of the system and Z is the charge of the nucleus. In hyperspherical coordinates, the Schrödinger equation for the rescaled wave function $\psi = R^{3/2} r_1 r_2 r_3 r_4 \Psi$ is written as

$$\left(-\frac{1}{2}\frac{\partial^2}{\partial R^2}+H_{\mathrm{ad}}(\Omega;R)-E\right)\psi=0, \tag{4}$$

where E is the total energy measured from the four-electron ionization threshold. The adiabatic Hamiltonian $H_{\mathrm{ad}}(\Omega;R)$ is an operator in Ω which depends parametrically on R, namely,

$$H_{\mathrm{ad}}(\Omega;R)=-\frac{\Lambda^2(\Omega)}{2R^2}+\frac{3}{8R^2}+\frac{C(\Omega)}{R}. \tag{5}$$

Here, $\Lambda^2(\Omega)$ is the square of the rescaled grand angular momentum operator. In the s^4 configuration, its explicit forms in the H set and the K set are

$$\Lambda^2(\Omega_{\rm H}) = \frac{1}{\sin\gamma\cos\gamma}\frac{\partial}{\partial\gamma}\sin\gamma\cos\gamma\frac{\partial}{\partial\gamma} + \frac{1}{\sin^2\gamma}\frac{\partial^2}{\partial\beta^2} + \frac{1}{\cos^2\gamma}\frac{\partial^2}{\partial\alpha^2} \tag{6}$$

and

$$\Lambda^2(\Omega_{\rm K}) = \frac{1}{\sin^2\gamma}\frac{\partial}{\partial\gamma}\sin^2\gamma\frac{\partial}{\partial\gamma} + \frac{1}{\sin^2\gamma\sin\beta}\frac{\partial}{\partial\beta}\sin\beta\frac{\partial}{\partial\beta} + \frac{1}{\sin^2\gamma\sin^2\beta}\frac{\partial^2}{\partial\alpha^2}, \tag{7}$$

respectively. $C(\Omega)$ is the effective charge representing the Coulombic potential energy among the electrons averaged over the s^4 configuration:

$$C(\Omega) = R\left(-\sum_{i=1}^{4}\frac{Z}{r_i} + \sum_{i<j}\frac{1}{(r_{ij})_>}\right), \tag{8}$$

where $(r_{ij})_>$ means the greater of r_i and r_j. The total wave function, with total spin S, which satisfies the Pauli principle, can be written as

$$\psi^S = \sum_\mu F_\mu^S(R)\left(\sum_{S_k}\Phi_\mu^{S,S_k}(\Omega;R)\chi_{S_k}^S\right), \tag{9}$$

where $F_\mu(R)$ is the hyperradial wave function and $\Phi_\mu^{S,S_k}(\Omega;R)$ the adiabatic channel function, and $\chi_{S_k}^S$ is the four-electron spin function with $S_k=\{S_{12},S_{12,3}\}$ or $\{S_{12},S_{34}\}$ representing a set of intermediate coupled spins, namely,

$$\chi_{\{S_{12},S_{12,3}\}} = (\{[\chi(1)\chi(2)]^{S_{12}}\chi(3)\}^{S_{12,3}}\chi(4))^S \tag{10}$$

or

$$\chi_{\{S_{12},S_{34}\}}^S = (\{[\chi(1)\chi(2)]^{S_{12}}[\chi(3)\chi(4)]^{S_{34}}\})^S. \tag{11}$$

The adiabatic potential $U_\mu(R)$ and its associated channel function $\Phi_\mu(\Omega;R)$ are obtained by solving the eigenvalue problem at each fixed R,

$$[H_{\rm ad}(\Omega;R) - U_\mu(R)]\Phi_\mu(\Omega;R) = 0. \tag{12}$$

We solve the three-dimensional eigenvalue problem, Eq. (12), numerically using direct products of discrete variable representation (DVR) basis sets [31] in the $1/8$ space of the hyperangles (α,β,γ) in the H set.

In Eq. (9), the summation inside the large parentheses is taken over all the possible intermediate spin states. Indeed, there are two intermediate spin states for spin singlet ($S=0$) states, and they are represented by using the coupling scheme $S_k=\{S_{12},S_{12,3}\}$ as

$$\chi_{\{S_{12},S_{12,3}\}}^S = \begin{cases}\chi_{\{0,1/2\}}^0,\\ \chi_{\{1,1/2\}}^0,\end{cases} \tag{13}$$

or by using $S_k=\{S_{12},S_{34}\}$ as

$$\chi_{\{S_{12},S_{34}\}}^S = \begin{cases}\chi_{\{0,0\}}^0,\\ \chi_{\{1,1\}}^0.\end{cases} \tag{14}$$

Similarly, for triplet ($S=1$) states, there are three independent intermediate spin states as

$$\chi_{\{S_{12},S_{12,3}\}}^S = \begin{cases}\chi_{\{0,1/2\}}^1,\\ \chi_{\{1,1/2\}}^1,\\ \chi_{\{1,3/2\}}^1,\end{cases} \tag{15}$$

or

$$\chi_{\{S_{12},S_{34}\}}^S = \begin{cases}\chi_{\{1,0\}}^1,\\ \chi_{\{1,1\}}^1,\\ \chi_{\{0,1\}}^1.\end{cases} \tag{16}$$

For quintet ($S=2$) states, there is only one type,

$$\chi_{\{S_{12},S_{12,3}\}}^S = \chi_{\{1,3/2\}}^2 \tag{17}$$

or

$$\chi_{\{S_{12},S_{34}\}}^S = \chi_{\{1,1\}}^2. \tag{18}$$

We note that spin states with different coupling schemes having the same total spin S are related via the following unitary transformation:

$$\chi_{\{1,1\}}^2 = \chi_{\{1,3/2\}}^2,$$

$$\chi_{\{1,0\}}^1 = \sqrt{\frac{2}{3}}\chi_{\{1,3/2\}}^1 - \sqrt{\frac{1}{3}}\chi_{\{1,1/2\}}^1,$$

$$\chi_{\{1,1\}}^1 = \sqrt{\frac{1}{3}}\chi_{\{1,3/2\}}^1 + \sqrt{\frac{2}{3}}\chi_{\{1,1/2\}}^1,$$

$$\chi_{\{0,1\}}^1 = \chi_{\{1,3/2\}}^1,$$

$$\chi_{\{0,0\}}^0 = \chi_{\{0,1/2\}}^0,$$

$$\chi_{\{1,1\}}^0 = \chi_{\{1,1/2\}}^0.$$

To satisfy the Pauli principle which requires that the total wave function ψ^S be antisymmetric under any pairs of electron exchange, the $\chi_{S_k}^S$ and Φ_μ^{S,S_k} are chosen such that they transform as basis functions for an irreducible representation and its conjugate representation of the symmetry group S_4, respectively [33]. In principle, the Hamiltonian matrix can be reduced by $1/24$, applying the proper symmetry of the S_4 group. However, as described in the previous section, we can only reduce the Hamiltonian matrix by $1/8$ with the exchange symmetries of (12), (34), and (13) and (24) in the H-set coordinates, and then sort out the wave functions with appropriate symmetries. This technique has been used for calculating the three-electron wave functions [26,34]. Indeed, applying the following boundary conditions:

$$(12)\Phi(\Omega;R) = -\Phi(\Omega;R),$$

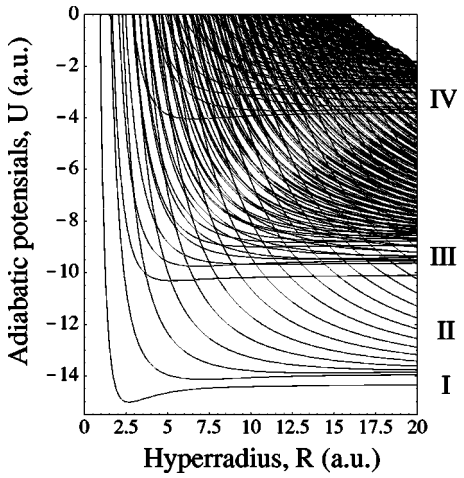

FIG. 3. Hyperspherical potentials for Be ($^1S^e$).

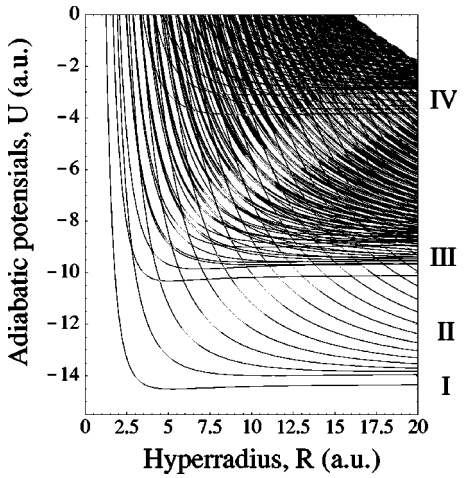

FIG. 4. Hyperspherical potentials for Be ($^3S^e$).

$$(34)\Phi(\Omega;R) = -\Phi(\Omega;R), \tag{19}$$

$$(13)(24)\Phi(\Omega;R) = +\Phi(\Omega;R),$$

we obtain two types of singlet ($S=0$) states associated with $\chi^S_{\{S_{12},S_{34}\}}=\chi^0_{\{1,1\}}$ and of quintet ($S=2$) states associated with $\chi^S_{\{S_{12},S_{34}\}}=\chi^2_{\{1,1\}}$ together. We cannot separate these two symmetries based on the boundary conditions in Eq. (19). Thus, we sort out the quintet and the singlet states, by applying the projection operators of the S_4 group,

$$P^S_{S_k,S'_k} = \sum_i D^S_{S_kS'_k}(p_i)p_i, \tag{20}$$

to the calculated eigenfunctions in the $1/8$ space. Here p_i is the ith permutation operator of the S_4 group, and $D^S_{S_kS'_k}(p_i)$ is the $\{S_k,S'_k\}$th matrix element of the irreducible representation associated with total spin S. Similarly, with the set of boundary conditions

$$(12)\Phi(\Omega;R) = -\Phi(\Omega;R),$$

$$(34)\Phi(\Omega;R) = -\Phi(\Omega;R), \tag{21}$$

$$(13)(24)\Phi(\Omega;R) = -\Phi(\Omega;R),$$

we obtain only triplet ($S=1$) states associated with $\chi^S_{\{S_{12},S_{34}\}}=\chi^1_{\{1,1\}}$. The states associated with all other symmetries such as totally symmetric functions are also obtained by using a similar set of boundary conditions as in Eq. (19) and the projection operator of the form in Eq. (20).

III. HYPERSPHERICAL ANALYSIS OF FOUR-ELECTRON ATOMS IN THE s^4 CONFIGURATION

The potential curves

In this subsection, we first present adiabatic potentials of the Be atom within the s^4 configuration. The adiabatic hyperspherical potential curves for $S=0$, 1, and 2 are shown in Figs. 3–5, respectively. The general features of the potential curves are almost the same as those of two- and three-electron atoms. At small R, each potential curve goes up as $1/R^2$ due to the dominance of the kinetic energy in R, which is controlled by the grand angular momentum. At large R, where the Coulomb potential energy dominates, each curve approaches one of the three-electron Be^+ states asymptotically and varies with R as $-1/R$. In the intermediate region, each curve has the form of a potential well where bound states or resonances can be formed. Let us examine in more detail the two limits of $R\to 0$ and $R\to\infty$. At small R, the Coulombic potential becomes negligible, and the adiabatic Hamiltonian approaches

$$H_{\rm ad}(\Omega;R) \to \frac{\Lambda^2(\Omega)/2+3/8}{R^2}. \tag{22}$$

Thus each potential goes up at small R as

$$U_\mu(R) \to \frac{\lambda(\lambda+10)/2+12+3/8}{R^2}, \tag{23}$$

where $\lambda=4,6,8,\ldots$ for s^4 configuration [28]. Meanwhile, in the large R limit, one electron is far away from the other electrons and the nucleus. The K-set coordinates are convenient to analyze the system at the large R limit. Introducing

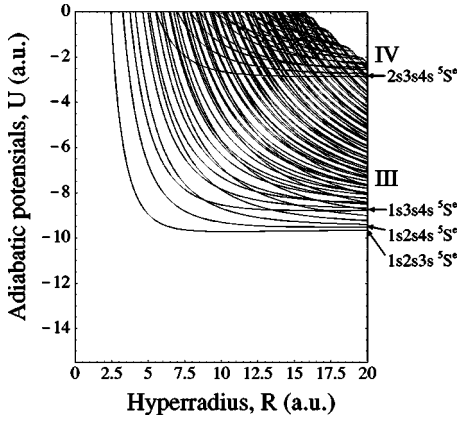

FIG. 5. Hyperspherical potentials for Be ($^5S^e$).

the hyperradius of a three-electron subsystem, $\rho = \sqrt{r_1^2+r_2^2+r_3^2} = R \sin\gamma$, the adiabatic Hamiltonian in the region of $(r_1, r_2, r_3) \leqslant r_4$ can be expressed as

$$H_{\rm ad}(\Omega_{\rm K}; R) = H^{3e}(\alpha, \beta, \rho) - \frac{Z-3}{R}\left[1 - \left(\frac{\rho}{R}\right)^2\right]^{-1/2}, \quad (24)$$

where H^{3e} is the Hamiltonian of the three-electron subsystem,

$$H^{3e}(\alpha,\beta,\rho) = -\frac{1}{2\rho}\frac{\partial^2}{\partial\rho^2}\rho - \frac{1}{2\rho^2}\left[\frac{1}{\sin\beta}\frac{\partial}{\partial\beta}\sin\beta\frac{\partial}{\partial\beta} + \frac{1}{\sin^2\beta}\frac{\partial^2}{\partial\alpha^2}\right] + \frac{C_{3e}(\alpha,\beta)}{\rho}, \quad (25)$$

and

$$C_{3e}(\alpha,\beta) = \rho\left(-\sum_{i=1}^{3}\frac{Z}{r_i} + \sum_{i<j}\frac{1}{(r_{ij})_>}\right) \quad (26)$$

is the effective charge for the three-electron atom with the nuclear charge Z. Except for the screened Coulombic potential and the quadrupolelike term, the adiabatic Hamiltonian for a four-electron atom coincides with the three-electron Hamiltonian. Thus, each adiabatic potential approaches one of the Be^+ ionic states as $-1/R$ at large R.

We have separated the curves into subgroups by their asymptotic limits at $R \to \infty$. Let us first analyze the singlet potential curves (see Fig. 3). There are four groups. The first group, labeled as I, consists of only one curve. This curve converges to the ground state of Be^+ $(1s^2 2s\ ^2S^e)$. The binding energies and wave functions of the ground state, designated as $1s^2 2s^2\ ^1S^e$, and singly excited states, designated as $1s^2 2sns\ ^1S^e$ $(n \geqslant 3)$, of the Be atom can be evaluated approximately using this potential. The binding energy calculated from the single-channel adiabatic approximation including the second order derivative term is −14.616 a.u., which is slightly higher than the result of the nonrelativistic variational calculation, −14.667 355 5 a.u. [32], but is lower than that of the Hartree-Fock approximation, −14.5303 a.u. More accurate result can be obtained by including the coupling with the higher channels and with basis sets that have higher angular momenta. The next group of curves, labeled II in the figure, approach the singly excited states of Be^+ $(1s^2 ms\ ^2S^e, m \geqslant 3)$ and they support doubly excited states of Be. The lowest curve of this group supports $(1s^2 3s\ ^2S^e)ns\ ^1S^e$ states. The higher curves of this group II support higher doubly excited states of the type $(1s^2 ms\ ^2S^e)ns\ ^1S^e$ for $n \geqslant m \geqslant 3$. The next group of curves are labeled III. They converge to the doubly excited states of Be^+ $(1sksms, m \geqslant k \geqslant 2)$ and they support triply excited states. The lowest curve of this group would support $(1s2s^2\ ^2S^e)ns\ ^1S^e$ $(n \geqslant 3)$ triply excited states. These triply excited states have a hole in the K shell. In other words, one electron is in the 1s shell and the other three are all in a higher orbital of $n \geqslant 2$. The last group of curves, labeled IV, approach the triply excited states of Be^+ $(jsksms\ ^2S^e)$ and they are to support quadruply excited states of Be of the types $jsksmsns\ ^1S^e$ $(2 \leqslant j \leqslant k \leqslant m \leqslant n)$. Figure 3 illustrates that all the eigenstates of a four-electron atom are obtained simultaneously using the hyperspherical approach. Similar potential curves have been assigned for singly, doubly, triply, and quadruply excited states for $S=1$ in Fig. 4. The lowest potential for $S=1$ is much shallower than that for the $S=0$ symmetry, since the lowest state for $S=1$ is $1s^2 2s 3s\ ^3S^e$ due to the Pauli principle. For $S=2$, the spins of all the four electrons are aligned such that the lowest state would be $1s2s3s4s\ ^5S^e$. Thus there are no singly and doubly excited states, and the potential curves in Fig. 5 do not include types I and II.

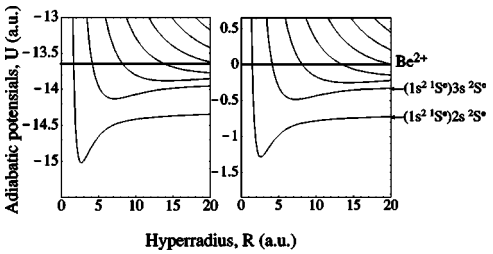

FIG. 6. Comparison of four-electron hyperspherical potentials of Be $(s^4\ ^1S^e)$ to the two-electron hyperspherical potentials with a model potential. The parameters for the model potential are the same as those used in Ref. [37]. Note that the hyperradius is defined by $R = \sqrt{r_1^2+r_2^2}$ for the two-electron model.

We next examine the $^1S^e$ potential curves that support singly (I) and doubly (II) excited states more carefully. The first few curves of Fig. 3 are shown in Fig. 6. Since the configurations of the two inner electrons are $1s^2\ ^1S^e$ for all these states, we can treat the two inner electrons as frozen and consider the two outer electrons only. In other words, for the singly and doubly excited states of Be, it is possible to carry out a two-electron atomic calculation by freezing the two 1s electrons and treat the two outer electrons in a model potential [35–38]. The potential curves calculated in hyperspherical coordinates for such a two-valence-electron system within the s^2 configuration are shown in Fig. 6. Clearly the two sets of potential curves are very similar. Thus the doubly excited states of a four-electron atom can be classified using the same set of quantum numbers that describe the doubly excited states of a two-electron atom. Note that the potentials calculated using the real four-electron atomic Hamiltonian do not contain the so called "ghost channel" which appears in the model two-electron atom.

In Fig. 7 we zoom in the curves of type III that support triply excited states. These curves are intersected by the family of curves that support doubly excited states. The curves for the latter are almost like vertical straight lines in the region considered and their crossings with the curves for the triply excited states are very sharp, indicating that there are little interactions among the curves from the different groups. The lowest curve in type III supports the $\{(1s2s\ ^1S^e)2s\ ^2S^e\}ns\ ^1S^e$ $(n \geqslant 3)$ triply excited states, while the next two curves support $\{(1s2s\ ^{1,3}S^e)3s\ ^2S^e\}ns\ ^1S^e$ triply excited states. In the asymptotic region, the two curves of the $\{(1s2s\ ^{1,3}S^e)3s\ ^2S^e\}ns\ ^1S^e$ states are separated by the exchange interaction energy between the 1s and 2s electrons. The lowest state of the singlet grandparent is $\{(1s2s\ ^1S^e)3s\ ^2S^e\}3s\ ^1S^e$, while that of the triplet grandparent

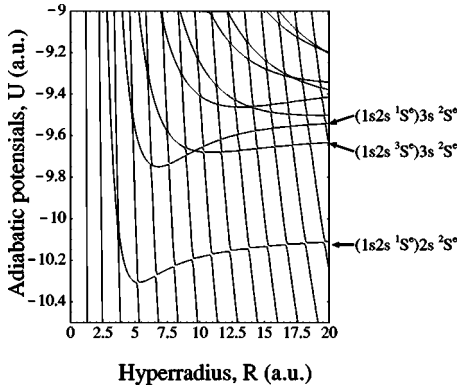

FIG. 7. Hyperspherical potentials of Be ($^1S^e$) in the energy region of the triply excited states.

is $\{(1s2s\ ^3S^e)3s\ ^2S^e\}4s\ ^1S^e$. That is, the intrashell state of two outer electrons is allowed for the singlet grandparent core and thus the potential curve is more attractive even though its potential curve lies above the triplet grandparent one at large R. Consequently, the two sets of curves cross each other. Since the crossing is quite sharp, the singlet-triplet grandparent mixing is weak and the triply excited states can be approximately labeled with singlet or triplet grandparents. In addition to the singlet or triplet grandparents, these triply excited states can be classified similarly to the triply excited states of a three-electron atom [16,17].

Finally, we come to address quadruply excited states. The potential curves supporting such states can be discerned from Fig. 8. These curves have numerous sharp avoided crossings with curves that support doubly and triply excited states. We have labeled the first few curves using the triply excited state core that these quadruply excited states are attached to, where the triply excited states are labeled using the IPM. One can see the hierarchical order of the levels of quadruply excited states. Thus the lowest quadruply excited Rydberg series is the one formed with the three-electron core $(2s^2\ ^1S^e)3s\ ^2S^e$. The next series is the one with identical grandparent $2s^2\ ^1S^e$ but the third electron is excited to $4s$. Clearly each $(2s^2\ ^1S^e)ns\ ^2S^e$ core has its own quadruply excited Rydberg series. The next subgroup of quadruply excited states would have excited grandparents, i.e., the first

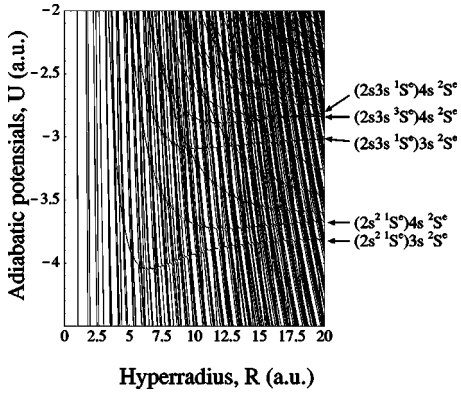

FIG. 8. Hyperspherical potentials of Be ($^1S^e$) in the energy region of the quadruply excited states.

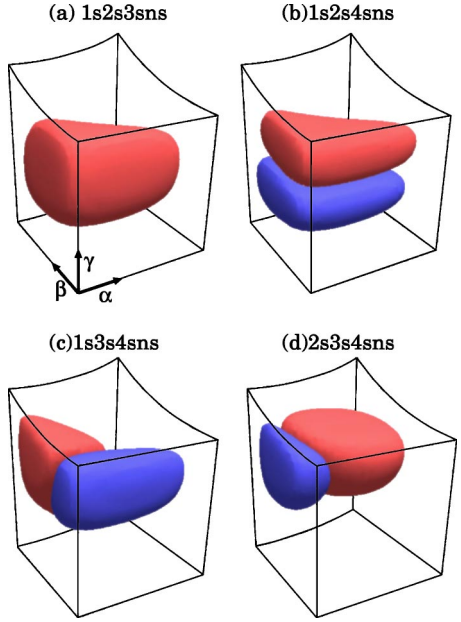

FIG. 9. Nodal structures of hyperspherical channel functions for $^5S^e$ sates in (α,β,γ) at $R=10$ a.u. (a) $1s2s3sns$, (b) $1s2s4sns$, (c) $1s3s4sns$, and (d) $2s3s4sns$. Each function is plotted in the domain of $r_1 \leqslant r_2 \leqslant r_3 \leqslant r_4$ in K-set coordinates; see Fig. 2(c).

two electrons form $2s3s$, in either the singlet or triplet two-electron core, before coupling to the third outer electron.

From these potential curves it is clear that within the s^4 configuration, the singly, doubly, triply, and quadruply excited states of a four-electron atom can indeed be all calculated at the same time. By removing the s^4 restriction, clearly there will be more potential curves for each group. For the purpose of analyzing the nature of the wave functions of these states, the s^4 model allows us to examine the nature of radial correlation. This is the subject of the next subsection.

IV. HYPERSPHERICAL ADIABATIC CHANNEL FUNCTIONS

In order to identify the features that characterize the adiabatic channels of a four-electron atom, we examine the channel functions $\Phi_\mu(\Omega;R)$. We will focus on quintet $(S=2)$ states only. For $S=2$ states, there is only one intermediate spin state corresponding to a quartet parent $(S_{12,3}=3/2)$ and a triplet grandparent $(S_{12}=1)$, and the full spin function is totally symmetric such that the spatial wave function is antisymmetric under electron permutations. Thus, the spatial wave function should vanish on each of the boundary surfaces of the domain in Fig. 2(b), and the number of nodal surfaces is the same in each of the 24 domains.

In Fig. 9, we show the channel functions $\Phi(\Omega_K;R)$ in the region of $r_1 \leqslant r_2 \leqslant r_3 \leqslant r_4$, as displayed in Fig. 2(c). The value of R is fixed at 10 a.u. To highlight the nodal surfaces of the channel functions, we will show the contour surface where the absolute value of the channel function is 10% of the maximum of the absolute value. Different shading is used to distinguish the region where the wave function has "+" phase vs the "−" phase. A contour surface of slightly higher

absolute value would fit inside the surface, but the nodal structures would stay the same. The nodal structures of the channel functions evolve smoothly as the value of R is changed except in localized regions where the adiabatic potential curves exhibit avoided crossings. Thus it is enough to analyze the nodal structures at one of the fixed values of R only.

The channel function associated with the lowest potential curve in Fig. 5, which supports the $1s2s3sns$ series, should have no nodes within the domain. This is clearly seen in Fig. 9(a). The surface is also very smooth and the wave function is distributed with its maximum near the center of the domain, when the value of $R \sim 10$ a.u. Note that in general, as R increases, the functions move to the corner of $(\alpha, \beta, \gamma) = (0, 0, 0)$ where the Coulomb potential is more attractive. Recall that the radial excitation of the outermost electron is represented by the distribution in the hyperradius R. Thus the Rydberg states in the $1s2s3sns$ series are distinguished by the number of nodes in $F(R)$ within the adiabatic approximation.

The channel function for the second lowest channel associated with each of the $1s2s4sns$ states is depicted in Fig. 9(b). This function clearly has a node which is almost perpendicular to the γ axis, and the (α, β) dependence of the function is very similar to the lowest channel for the $1s2s3sns$ states in Fig. 9(a). Clearly, using the K-set coordinates in the region of $r_1 \leqslant r_2 \leqslant r_3 \leqslant r_4$, the radial excitation of the third innermost electron is determined by the nodal surfaces in hyperangle γ. Following this procedure, each of the $1s2s5sns$ states, where the $5s$ state for the third innermost electron has one more quantum of radial excitation than the $4s$ state, the channel function would have two nodal surfaces at two values of $\gamma \simeq$ const. Increasing the radial excitation of the third electron increases the number of nodes in γ.

Next, for $1s3s4sns$ states, where the second innermost electron is also excited, the channel function is shown in Fig. 9(c). There is a different nodal surface given approximately by $\beta \simeq$ const. Similar to the nodes in γ, the radial excitation of the second innermost electron is characterized by the nodal surfaces in β, and increasing the radial excitation of the second electron increases the number of nodes in β. We notice that the nodal surface is not very flat comparing to the node in γ in Fig. 9(b). The node in Fig. 9(c) changes gradually only in β when γ is changed. This indicates that the motion in γ can be fixed when we consider the motion in β, namely, the adiabatic Hamiltonian expressed in Eqs. (24) and (25) can be approximately solved with γ fixed, and the motion in β is regarded as "faster" than that in γ, in the hierarchical adiabatic order as for the three-electron atoms [26].

Proceeding further, examination of the channel function for the $2s3s4sns$ quadruply excited states shows that there is another nodal surface in $\alpha \simeq$ const, implying that the radial excitations of the innermost electron are represented by nodes in α. The plot also shows a larger deviation from a flat surface comparing to those of the nodes in β and γ. This implies that the motion in α is regarded as "fastest" among the hyperspherical variables.

We can summarize that within the hyperspherical approach, the radial function of the outermost electron is characterized by the hyperradius R where the degree of excitation is determined by the number of hyperradial nodes. Similarly, the radial excitation of the third innermost electron is characterized by the angle γ, the second innermost electron by β, and the innermost electron by α. The motions in these hyperspherical variables fit the hierarchical adiabatic picture: The motion of outer electron can indeed be regarded as slower than that of the inner one. This is possible only because we used the angles in the K-set coordinate to characterize each electron in the domain of $r_1 \leqslant r_2 \leqslant r_3 \leqslant r_4$.

V. SUMMARY AND CONCLUSION

In this paper we examine the radial correlation of a four-electron model atom by assuming that each electron has zero orbital angular momentum. Within this configuration we have four degrees of freedom and hyperspherical coordinates were used for such a study. There are two sets of hyperangles that are convenient to parameterize the coordinate space. One is the H set and the other the K set. We have solved the Schrödinger equation in the H set, since the symmetry imposed by these identical particles is easier to implement in this set. To display the resulting wave functions it is more convenient to express in K-set coordinates. The adiabatic hyperspherical potential curves have been calculated in the s^4 configuration for total spin $S=0$, 1, and 2. We have found that potential curves for the singly, doubly, triply, and quadruply excited states in the s^4 configuration can be identified (see Figs. 3–5). We have also analyzed the channel functions to show that multiply excited states can be classified with the number of nodes in the hyperangles α, β, and γ, in the K-set coordinates.

The results obtained in this paper is to show *in principle* how to study quadruply excited states of a four-electron atom. The s^4 model has all the key elements that allow us to distinguish the major characteristics of singly, doubly, triply, and quadruply excited states. This model complements with the other model where the four electrons are confined to the surface of a sphere that is appropriate for studying angular correlations in intrashell quadruply excited states. To treat realistic four-electron atoms the present approach has to be extended to including states where the orbital angular momentum of each electron is not zero. There is no built-in difficulty for such an extension from the computational viewpoint. However, the number of channels for quadruply excited states is quite large for each symmetry. There is also the essential difficulty in examining the radial and angular correlations together in each wave function. Even within the adiabatic approximation within the hyperspherical approach, each channel wave function is still represented by a function of eight variables after the rotational motion of the whole atom is removed. Thus the eventual classification of these states would have to rely on the partial display of the channel function in some subspace. We do not expect that this goal can be reached any time soon, but the present work has laid down the theoretical and computational procedure for such studies in the future based on the hyperspherical coordinates.

ACKNOWLEDGMENTS

T.M. wishes to thank Professor M. Matsuzawa and Professor S. Watanabe for their encouragement throughout this

work. T.M. was supported in part by a Grant-in-Aid for Young Scientists (B) from the Japan Society for the Promotion of Science, by a Grant-in-Aid for Scientific Research (C) from the Ministry of Education, Culture, Sports, Science and Technology, Japan, and by the 21st Century COE program on "Coherent Optical Science." T.M. also received financial aid from the Matsuo Foundation. C.D.L. was supported in part by Chemical Sciences, Geosciences and Biosciences Division, Office of Basic Energy Sciences, Office of Science, U.S. Department of Energy.

[1] J. W. Cooper, U. Fano, and F. Prats, Phys. Rev. Lett. **10**, 518 (1963).
[2] D. R. Herrick and O. Sinanoğlu, Phys. Rev. A **11**, 97 (1975).
[3] M. E. Kellman and D. R. Herrick, J. Phys. B **11**, L755 (1978).
[4] O. Sinanoğlu and D. R. Herrick, J. Chem. Phys. **62**, 886 (1975).
[5] M. E. Kellman and D. R. Herrick, Phys. Rev. A **22**, 1536 (1980).
[6] G. S. Ezra and R. S. Berry, Phys. Rev. A **28**, 1974 (1983).
[7] C. D. Lin, Adv. At. Mol. Phys. **22**, 27 (1986).
[8] S. Watanabe and C. D. Lin, Phys. Rev. A **34**, 823 (1986).
[9] J. M. Feagin and J. S. Briggs, Phys. Rev. Lett. **57**, 984 (1986).
[10] J. M. Rost, K. Schulz, M. Domke, and G. Kaindl, J. Phys. B **30**, R4663 (1997).
[11] G. Tanner, K. Richter, and J. M. Rost, Rev. Mod. Phys. **72**, 497 (2000).
[12] S. Watanabe and C. D. Lin, Phys. Rev. A **36**, 511 (1987).
[13] C. G. Bao, X. Yang, and C. D. Lin, Phys. Rev. A **55**, 4168 (1997).
[14] T. Morishita, Y. Li, and C. D. Lin, Phys. Rev. A **58**, 4214 (1998).
[15] T. Morishita and C. D. Lin, Phys. Rev. A **59**, 1994 (1999).
[16] T. Morishita and C. D. Lin, Phys. Rev. A **64**, 052502 (2001).
[17] T. Morishita and C. D. Lin, Phys. Rev. A **67**, 022511 (2003).
[18] L. B. Madsen, J. Phys. B **36**, R223 (2003).
[19] Y. Azuma and S. Hasegawa (private communication).
[20] C. G. Bao, J. Phys. B **26**, 4671 (1993).
[21] C. G. Bao, Phys. Rev. A **47**, 1752 (1993).
[22] C. G. Bao and Y. W. Duan, Phys. Rev. A **49**, 818 (1994).
[23] C. G. Bao, Phys. Rev. A **50**, 2182 (1994).
[24] Y. Komninos and C. A. Nicolaides, Phys. Rev. A **50**, 3782 (1994).
[25] X. Yang, J. Xi, C. G. Bao, and C. D. Lin, Phys. Rev. A **52**, 2029 (1995).
[26] T. Morishita, O. I. Tolstikhin, S. Watanabe, and M. Matsuzawa, Phys. Rev. A **56**, 3559 (1997).
[27] N. Berrah, J. D. Bozek, A. A. Wills, G. Turri, H.-L. Zhou, S. T. Manson, G. Akerman, B. Rude, N. D. Gibson, C. W. Walter, L. Voky, A. Hibbert, and S. M. Ferguson, Phys. Rev. Lett. **87**, 253002 (2001).
[28] M. Cavagnero, Phys. Rev. A **30**, 1169 (1984).
[29] M. Cavagnero, Phys. Rev. A **33**, 2877 (1986).
[30] M. Cavagnero, Phys. Rev. A **36**, 523 (1987).
[31] D. O. Harris, G. G. Engerholm, and W. D. Gwinn, J. Chem. Phys. **43**, 1515 (1965); A. S. Dickinson and P. R. Certain, *ibid.* **49**, 4209 (1968); J. C. Light and R. B. Walker, *ibid.* **65**, 4272 (1976); J. C. Light, I. P. Hamilton, and J. V. Lill, *ibid.* **82**, 1400 (1985).
[32] J. Komasa, J. Rychlewski, and K. Jankowski, Phys. Rev. A **65**, 042507 (2002).
[33] M. Kotani, A. Amemiya, E. Ishiguro, and T. Kimura, *Table of Molecular Integrals* (Maruzen Co., Tokyo, 1955).
[34] T. Morishita and C. D. Lin, Phys. Rev. A **57**, 4268 (1998).
[35] C. D. Lin, J. Phys. B **16**, 723 (1983).
[36] C. H. Greene, Phys. Rev. A **23**, 661 (1981).
[37] B. Zhou and C. D. Lin, Phys. Rev. A **51**, 1286 (1995).
[38] S. Watanabe and T. Ebara, Phys. Rev. A **55**, 175 (1997).